$GdCl_3$ suppresses the malignant potential of hepatocellular carcinoma by inhibiting the expression of CD206 in tumor-associated macrophages

FANGYU ZHU[1,2], XIANGNAN LI[2], YONG JIANG[2], HAORAN ZHU[2], HAOLONG ZHANG[1], CHENGYAO ZHANG[1], YU ZHAO[1] and FANG LUO[2]

Departments of [1]Vascular Surgery, and [2]Hepatobiliary Surgery, The First Affiliated Hospital of Chongqing Medical University, Chongqing 400016, P.R. China

Received May 18, 2015; Accepted July 6, 2015

DOI: 10.3892/or.2015.4268

Abstract. In the present study, we aimed to ascertain whether there is a correlation between CD206 expression in tumor associated-macrophages (TAMs) and the prognosis of primary hepatocellular carcinomas (HCC) and we investigated the effect of $GdCl_3$ on HCC. The expression of CD206 in HCC tumor tissues and peri-carcinoma tissues was measured using an array for liver tissues. The effects of $GdCl_3$ on CD206 expression were examined in stimulated RAW264.7 cells. Target gene expression was evaluated by RT-PCR, western blotting and immunohistochemistry. The Transwell system was used to assess the invasiveness of HCC cells. Finally, we established a mouse model for HCC using N-nitrosodiethylamine (DEN) to determine the effect of $GdCl_3$ on HCC. Liver tissue array analysis revealed that CD206 was highly expressed in the HCC tissues compared to the level in peri-carcinoma tissue. We found that $GdCl_3$ suppressed the expression of CD206 in the M2 macrophage phenotype of stimulated RAW264.7 cells with an IC_{10} value of 0.07 $\mu g/\mu l$. In addition, $GdCl_3$ also induced cell apoptosis in the RAW264.7 cells. Addition of $GdCl_3$ into the culture medium of RAW264.7 cells markedly reduced the invasive ability of Hepa1-6 cells compared to the control cells. Accordingly, $GdCl_3$ treatment increased the expression of the epithelial-mesenchymal transition (EMT)-related protein E-cadherin while expression of N-cadherin, TWIST and Snail was reduced in IL-4-stimulated cells. Moreover, $GdCl_3$ treatment inhibited HCC progression in DEN-induced HCC mice, possibly by downregulating CD206. Our findings indicate that CD206 is a potential biomarker for predicting HCC prognosis and that $GdCl_3$ suppresses HCC progression by downregulating the expression of CD206 in TAMs.

Correspondence to: Professor Fang Luo, Department of Hepatobiliary Surgery, The First Affiliated Hospital of Chongqing Medical University, Chongqing 400016, P.R. China
E-mail: luofangdoctor19@163.com

Abbreviations: DEN, N-nitrosodiethylamine; HCC, hepatocellular carcinoma; IL, interleukin; TAMs, tumor-associated macrophages; TNF-α, tumor necrosis factor-α

Key words: CD206, tumor-associated macrophages, $GdCl_3$, HCC, N-nitrosodiethylamine

Introduction

Hepatocellular carcinoma (HCC) is the most common type of human liver cancer and is associated with a high mortality rate (1). HCC normally develops from chronic inflammation in which tumor-associated macrophages (TAMs), a paradigm for polarized M2 mononuclear phagocytes, play a critical role in inflammatory processes and promote disease progression (2-4). TAMs mediate tumor cell migration, invasion, proliferation and trigger the malignant potential of HCC by activating certain intracellular signaling pathways (5-7).

Identification and manipulation of TAMs are essential to prevent the development of malignancy in HCC (8). Innovative strategies to inhibit the function of TAMs such as pharmacological inhibitors may provide new options for therapeutic intervention (9). However, apart from certain drugs used in the clinic such as trabectedin, (10) most of the reagents are still under pre-clinical investigation. Gadolinium chloride ($GdCl_3$) is an injectable MRI contrast agent used in the clinic (11-13) that is also widely used for macrophage blockage in animal experiments. This drug may have applications for TAM blockage in human cancers. However, despite accumulating evidence on the influence of $GdCl_3$ on macrophages, the molecular mechanism of $GdCl_3$ activity remains undefined (11-13).

CD206, also known as mannose receptor 1 (MRC1), is a phagocytic and endocytic receptor that can recognize carbohydrate ligands in target molecules. CD206 expression is correlated with the alternatively activated (M2) polarization of macrophages (14). In patients with advanced castrate-resistant prostate cancer, upregulated numbers of $CD14^+/CD206^+$ cells were found in metastatic lesions, suggesting that upregulated levels of CD206 expression may be correlated with tumor metastasis (15). Nevertheless, the effect of $GdCl_3$ on CD206 function and the role of CD206 in HCC remain unclear.

In the present study, 90 HCC cases were examined. The expression level of CD206 in tumor tissues and peri-carcinoma tissues was measured and the association between the CD206

level and HCC prognosis was determined. In addition, we also investigated the molecular mechanism of $GdCl_3$-mediated anticancer action *in vitro* and *in vivo*. Our findings support the notion that $GdCl_3$ may be a novel therapeutic option for the management of HCC by inhibiting CD206 expression in TAMs.

Materials and methods

Reagents. Rabbit anti-CD206 primary antibody was purchased from Abcam (Shanghai, China). Horseradish peroxidase (HRP)-conjugated anti-rabbit secondary antibody and DAB reagent were obtained from Dako (Glostrup, Denmark). Lipopolysaccharide (LPS) from *Escherichia coli* 011:B4, $GdCl_3$ [gadolinium (III) chloride hexahydrate], and N-nitrosodiethylamine (DEN) were obtained from Sigma-Aldrich (St. Louis, MO, USA). IL-4 (recombinant murine IL-4) was purchased from PeproTech (Rocky Hill, NJ, USA). Phycoerythin (PE)/Cy5-conjugated anti-mouse CD16/32 antibody and fluorescein isothiocyanate (FITC)-conjugated anti-mouse CD206 antibody were purchased from Tianjin Sungene Biotech Co., Ltd. (Tianjin China). The following antibodies were obtained from Santa Cruz Biotechnology (Santa Cruz, CA, USA): mouse anti-NOS2 antibody, mouse anti-CD206 antibody, anti-cleaved caspase-3 antibody, anti-arginase I antibody and anti-TWIST. The anti-Snail, anti-N-cadherin, anti-E-cadherin, anti-TGF-β1 and anti-phospho-Smad3 antibodies were purchased from Cell Signaling Technology (Danvers, MA, USA). The rat anti-mouse Alexa Fluor 488 secondary antibody was purchased from AbD Serotec (San Francisco, CA, USA). The following antibodies were obtained from Life Technologies (Carlsbad, CA, USA): Alexa Fluor 488 goat anti-rabbit, goat anti-rat and goat anti-mouse IgG (H+L), Alexa Fluor 594 goat anti-rabbit and goat anti-mouse IgG (H+L) antibody. PCR primers were synthesized by Takara Bio (Dalian, China). The Cell Counting Kit-8 (CCK-8), DAPI stain and the Griess reagent were obtained from the Beyotime Institute of Biotechnology (Haimen, China). The Annexin V/propidium iodide (PI) detection kit was purchased from Nanjing KeyGen Biotech., Co., Ltd. (Nanjing, China).

Analysis of CD206 expression in HCC tissue samples. The protocol for the present study was approved by the Ethics Committee of the Taizhou Hospital of the Zhejiang Province. Ninety HCC and 90 peri-carcinoma tissue samples were collected from primary HCC patients undergoing surgery at the Taizhou Hospital of Zhejiang Province, China, between January 2010 and September 2011 after obtaining informed consent. All patients were monitored until September 2013.

The expression of CD206 was determined using a liver tissue array [(liver,180)HLiv-HCC180Sur-03] according to the manufacturer's instructions (Shanghai Outdo Biotech Co., Ltd., Shanghai, China). Briefly, samples were deparaffinized, rehydrated, heated in citrate buffer (0.01 M, pH 6.0) and incubated in endogenous peroxidase (3% hydrogen peroxide solution). After blocking, the samples were incubated overnight with a rabbit anti-CD206 antibody at 4˚C, overnight. An HRP-conjugated anti-rabbit secondary antibody and DAB reagent were used for CD206 staining. Following this, all sections were double-stained with hematoxylin. Images were analyzed using Aperio ImageScope software. All sections were reviewed by two physicians in the Pathology Department of The First Affiliated Hospital of Chongqing Medical University. A semi-quantitative and subjective grading system that considered both the intensity of staining and the proportion of tumor cells that had an unequivocal positive reaction were used to analyze the slides. The staining intensity was graded according to the following criteria: 0, negative staining; 1, light yellow or light brown staining; 2, yellow or brown staining; 3, dark yellow or dark brown staining. The percentage of positive staining was graded as follows: 0, positive staining in <1% of cells; 1, positive staining in 1-25% of cells; 2, positive staining in 26-50% of cells; 3, positive staining in 51-75% of cells; 4, positive staining in >75% of cells. The staining index was calculated as the staining intensity multiplied by the percentage of positive staining. Low expression was identified with a score <6 and high expression was identified with a score 6-12.

Cell culture, M1 macrophage and M2 macrophage polarization. The macrophage-like, mouse RAW264.7 cell line and the mouse liver cancer cell line Hepa1-6 were used in the present study. Both cell lines were maintained in DMEM/F-12 culture medium containing 10% fetal bovine serum (FBS) and grown in a 5% CO_2-humidified incubator at 37˚C. The RAW264.7 cells were induced to transform into the M1 phenotype by stimulating them with LPS (2.5 μg/ml; 2 h) and were then transformed into the M2 phenotype by exposing them to 10 ng/ml IL-4 for 48 h as previously described (16). The polarization of M1 and M2 was then verified by flow cytometry, immunocytochemistry, RT-PCR, western blotting, and Griess assay for the expression of the following cell markers: iNOS (NOS2), Arg-1, CD16/32 and F4/80. Induced M1 and M2 macrophages were collected for further studies.

Effects of $GdCl_3$ on the proliferation and apoptosis of RAW264.7 macrophages. The CCK-8 assay was used to measure cell proliferation according to the manufacturer's instructions. RAW264.7 ($5x10^3$) cells/well seeded on a 96-well plate were treated with different concentrations of $GdCl_3$ (0, 0.01, 0.05, 0.1, 0.2, 0.4, 0.6, 0.8 or 1 μg/μl) for 12 h. Each treatment was performed in quadruplicate. The WST8 was then added into each well, and cells were cultured for another 3 h. Absorbance at 450 nm was measured using a microplate reader (xMark™ Microplate Spectrophotometer System; Bio-Rad Laboratories, Hercules, CA, USA). Data were analyzed using regression analysis with SPSS 21.0 software (17), and the IC_{10} concentration of $GdCl_3$ was determined. The cleaved caspase-3 level was also examined by immunocytochemistry and flow cytometry using Annexin V/PI staining.

Expression of CD206 in RAW264.7 cells and cd206 siRNA transduction. CD206 expression in M1 or M2 macrophages with or without $GdCl_3$ pretreatment was determined by western blotting, RT-PCR and immunocytochemistry. To downregulate CD206 expression, macrophages were seeded onto 6-well plates. CD206 small interference RNA (siRNA) (Santa Cruz Biotechnology) or negative control siRNA (siRNA-A) (Santa Cruz Biotechnology) were mixed with Lipofectamine 2000 transfection reagent (Invitrogen) in 200 μl serum-free culture

medium. The mixture was added onto the cells. After 6 h, the media were replaced. Forty-eight or 72 h after transfection, the downregulation of CD206 expression was determined.

Cell invasion assay. After the indicated treatments, RAW264.7 cells were co-cultured with Hepa1-6 cells for the determination of Hepa1-6 invasive capability. The invasive capacity of cells was analyzed using a Transwell-Matrigel system (BD Biosciences, San Jose, CA, USA): $3x10^4$ Hepa1-6 cells were suspended in serum-free culture medium and plated in the upper chamber which was coated with Matrigel. The lower chambers were pre-seeded with M1 or M2 macrophages with or without $GdCl_3$ and CD206 or control siRNAs. After a 48-h incubation at 37˚C, the number of invasive cells was determined using a microscope. Five fields were randomly selected, and the average number of invasive cells was calculated.

In vivo study. Two-week old male BALB/c mice were purchased from the Laboratory Animal Center of Chongqing Medical University. The animals were randomly divided into four groups with 30 animals each: control, DEN, DEN+$GdCl_3$ and $GdCl_3$. To establish the rodent primary HCC model, mice were administered an intraperitoneal injection of DEN (5 μg/g) on week 0 to induce HCC within 40 weeks (18). The mice in the DEN+$GdCl_3$ group received an intraperitoneal injection of $GdCl_3$ (10 μg/g) twice weekly, starting eight weeks after the DEN injection until the end of the study. Control animals were administered saline. In the $GdCl_3$ group, mice received $GdCl_3$ (10 μg/g) eight weeks after the first saline injection. The tumor volumes were calculated using the following equation: V = (length x width^2)/2. The tumor volume growth rate (TVGR) and tumor inhibition rate (TIR) were calculated using the following equations:

$$TVGR = (V_{DEN+GdCl_3}/V_{DEN}) \times 100\% \text{ (19);}$$

TIR = [(Average tumor weight of group DEN - Average tumor weight of group DEN+$GdCl_3$)/Average tumor weight of group DEN] x 100% (20).

The animal survival was analyzed using the Kaplan-Meier assay and the log-rank test.

Real-time quantitative PCR. Total RNA was extracted from cells or tissues using an RNAiso Plus extraction kit according to the manufacturer's instructions (Takara). RNA was reverse transcribed using the PrimeScript® RT Master Mix (Takara), and RT-PCR was performed using an ABI Prism® 7500 sequence detection system (Life Technologies). PCR amplification was carried out using SYBR® Premix DimerEraser™ (Takara) with the following primers: *cd206*, sense, CTCAACCCAAGGGCTCTTCTAA and antisense, AGGTGGCCTCTTGAGGTATGTG; *NF-κB*, sense, AGATGGCCGGTTCTAGAC and antisense, AGGTGGTTGGTGAGGTTGATG; *arg-1*, sense, CAGAAGAATGGAAGAGTCAG and antisense, CAGATATGCAGGGAGTCACC; *inos*, sense, CTGCAGCACTTGGATCAGGAACCTG and antisense, GGGAGTAGCCTGTGTGCACCTGGAA; *β-actin*, sense, GACCCAGATCATGTTTGAGACC and antisense, GCTAGGAGCCAGAGCAGTAATCT. Reaction conditions were as follows: 95˚C for 30 sec; 95˚C for 5 sec; 55˚C for 30 sec; 72˚C for 34 sec for 40 cycles. All amplifications were repeated three times. Relative expression from the amplified RNA samples was calculated using the $2^{-\Delta\Delta CT}$ method.

ELISA and biochemical assays. Animals were anesthetized with an intraperitoneal injection of 1% pentobarbital sodium and blood was collected by heart puncture. Blood serum was isolated by centrifugation and used for analysis. Tumor necrosis factor-α (TNF-α) and interleukin (IL)-6 levels in the mouse serum or the culture medium of macrophages were determined using an ELISA kit according to the manufacturer's instructions (Nanjing Jiancheng Bioengineering Institute, Nanjing, China). ALT and AST levels in blood serum were assessed using a Modular auto-biochemical analyzer (Hoffmann-La Roche, Basel, Switzerland).

Histology and immunohistochemistry. Mouse tumor samples were stained with 0.5% Sirius red (Sigma-Aldrich) and saturated with picric acid solution to study the fibrosis of the mouse liver tissue. For immunohistochemical analysis, the sections were incubated with primary antibodies for F4/80 (1:50), CD206 (1:50), cleaved caspase-3 antibody (1:400) or NOS2 (1:50) at 4˚C overnight. Samples were washed and incubated with Alexa Fluor 555 goat anti-rat and goat anti-mouse IgG (H+L) or Alexa Fluor 488 goat anti-rabbit and goat anti-rat IgG (H+L) secondary antibodies. Some samples were deparaffinized in xylene and rehydrated in an ethanol series. After blocking, the samples were probed with an anti-CD206 antibody (1:4,000) or an anti-CD31 antibody (1:50) at 4˚C overnight. Immunostaining was performed using an immunohistochemistry kit according to the manufacturer's instructions (Beijing Zhongshan Golden Bridge Biotechnology Co., Ltd., Beijing, China). Antibody binding was visualized using 3,3'-diaminobenzidine tetrahydrochloride (DAB). Images were analyzed using Image-Pro Plus software and the expression of CD31 was quantified using microvessel density (MVD) score (21).

Western blotting. Total protein was extracted and separated using sodium dodecyl sulfate-polyacrylamide gel electrophoresis (SDS-PAGE). Lysates were transferred onto a PVDF membrane (Millipore, Billerica, MA, USA). The membranes were blocked and incubated overnight with primary antibodies at 4˚C. Following washing, the membranes were incubated with HRP-labeled secondary antibodies. Bands were visualized using enhanced chemiluminescence (ECL) kits according to the manufacturer's instructions (Beyotime Institute of Biotechnology). Antibodies for β-actin and GAPDH were used as internal controls.

Statistical analysis. Data were analyzed using SPSS 21.0 software and GraphPad Prism 5. Statistical significance was determined using one-way analysis of variance (ANOVA), Student's t-test, Chi-square analysis, linear progression analysis, log-rank test, and COX association analysis. Data are presented as mean ± standard deviation (SD). $P<0.05$ was recognized as significantly different.

Results

A high level of CD206 expression correlates with poor survival of HCC patients. CD206 was highly expressed in

Table I. Relationship between CD206 expression and the clinical characteristics of the HCC cases (in HCC tumor tissue; para-HCC tumor tissue).

	HCC intratumoral			HCC peri-tumoral		
	CD206 expression			CD206 expression		
	High (12)	Low (78)	P-value	Positive (68)	Negative (22)	P-value
Gender						
Male	9	65	0.441	56	19	1.000
Female	3	13		12	3	
Age (years)						
≤65	8	73	0.016	56	19	1.000
>65	4	5		12	3	
Tumor size (cm)						
≤5	4	50	0.000	26	5	0.209
>5	18	28		42	17	
Pathological grading						
I	4	13	0.230	13	4	1.000
II-III	8	65		55	18	
TNM stage						
I/II	5	49	0.210	42	11	0.455
III/VI	7	29		26	11	
Tumor capsular						
Present	10	55	0.498	53	12	0.053
Absent	2	23		15	10	
Metastasis						
Yes	0	7	0.587	5	2	1.000
No	12	71		63	20	

Table II. Cox regression model.

	B	SE	Wald	df	Sig	Exp (B)
Pathological grading	0.371	0.184	4.085	1	0.043	1.449
TNM stage	0.750	0.303	6.113	1	0.013	2.117
Gender	1.276	0.543	5.528	1	0.019	3.581
HCC CD206	0.863	0.412	4.394	1	0.036	2.371

the HCC tissues compared with that in the peri-carcinoma tissues (Fig. 1A). Kaplan-Meier analysis with log-rank test demonstrated that patients with high CD206 expression in tumor tissues had a poorer prognosis than patients with low CD206 expression (P=0.008) (Fig. 1B). No significant differences was detected for peri-carcinoma tissues (P=0.772). Next, we examined the association between CD206 expression and the demographic and clinical characteristics of the HCC patients. As shown in Table I, patients ≤65 years of age or with a tumor size ≤5 cm had reduced levels of CD206 expression in HCC tissues (P<0.05). COX regression analysis indicated that the pathological grading (RR=1.449, P=0.043), TNM stage (RR=2.117, P=0.013), gender (RR=3.581, P= 0.019) and CD206 expression in tumors (RR=2.371, P=0.036) were independent factors associated with prognosis (Table II).

$GdCl_3$ suppresses CD206 expression and induces apoptosis of macrophages. LPS and IL-4 were used to stimulate the RAW264.7 macrophages to mature into M1 and M2 macrophages. Following LPS stimulation, expression of *iNOS*, *NF-κB*, and CD16/32 target genes was upregulated, whereas Arg-1 expression was downregulated (Fig. 2A-D). M2 macrophages have much higher levels of *CD206* and *Arg-1* than their M1 counterparts. These results confirmed that IL-4 induced an M2 macrophage phenotype in the RAW264.7 cells which have a higher CD206 expression level. To understand the effects

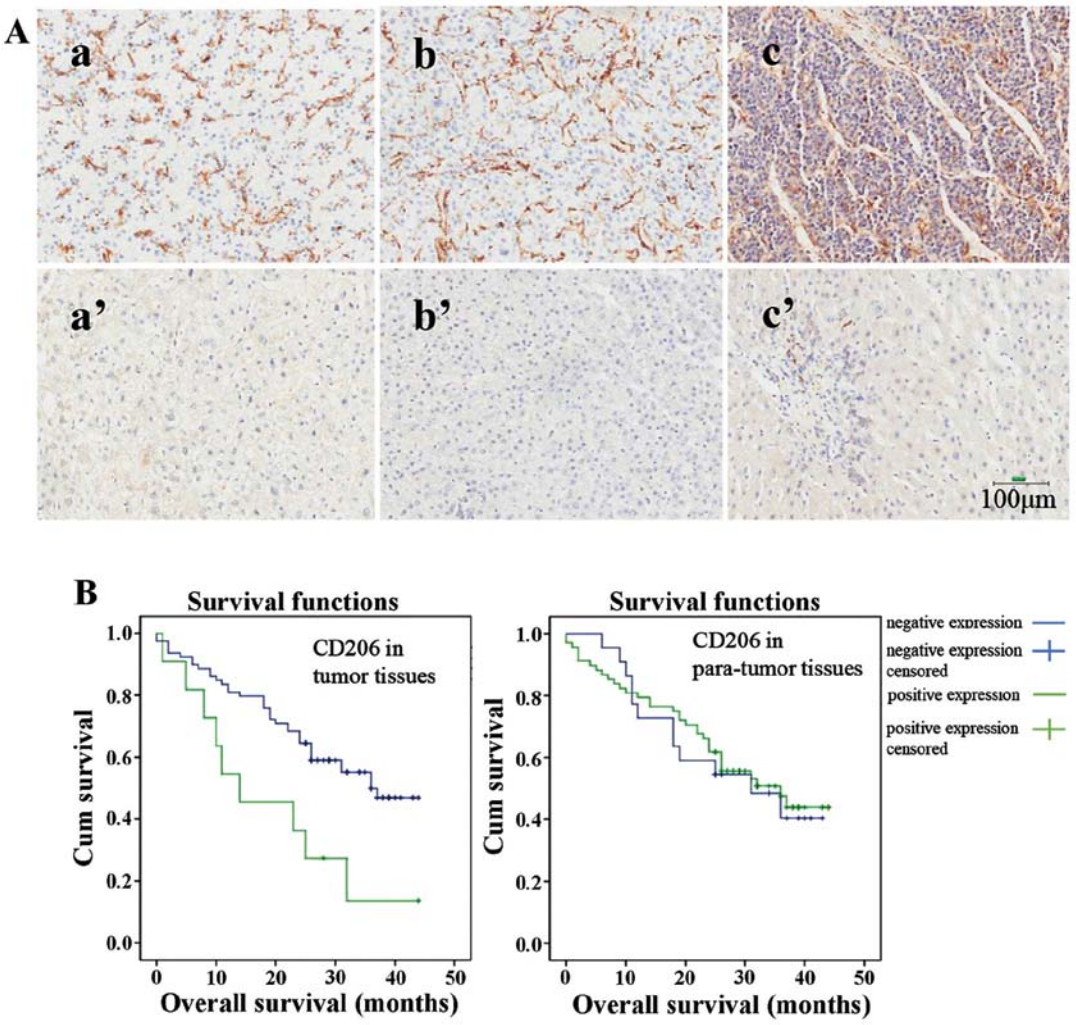

Figure 1. Association between CD206 expression in HCC and HCC patient survival. (A) Representative immunohistological data of CD206 staining. a, b and c were derived from three HCC tissues; a', b' and c' were derived from related peri-carcinoma tissues. Magnification, x200. Scale bar, 100 μm. (B) The association between CD206 expression and overall survival time. HCC tissues, n=90; peri-carcinoma tissues, n=90.

of $GdCl_3$ on RAW264.7 cells, CCK-8 assay was conducted. We found that $GdCl_3$ inhibited the proliferation of RAW264.7 cells in a dose-dependent manner. The IC_{10} and IC_{50} values of $GdCl_3$ treatment were 0.07 μg/μl (0.26 mM) and 0.19 μg/μl (0.71 mM), respectively. We found that at the lowest cell inhibition rate induced by 0.07 μg/μl $GdCl_3$ treatment, the CD206 expression in IL-4-stimulated cells was efficiently suppressed (P<0.001) (Fig. 2E-G).

We next investigated apoptosis in LPS- or IL-4-stimulated RAW264.7 cells following treatment with 0.07 μg/μl $GdCl_3$. As shown in Fig. 3A and B, $GdCl_3$ incubation induced apoptosis in both the LPS- and IL-4-stimulated RAW264.7 cells. However, 0.07 μg/μl $GdCl_3$ treatment did not induce significant apoptosis in liver hepatoma Hepa1-6 cells (Fig. 3C).

Downregulation of CD206 expression by $GdCl_3$ or cd206 siRNA results in reduced invasiveness of HCC cells. We next used the Transwell Matrigel assay to determine the role of CD206-expressed M2 macrophages on the invasiveness of HCC cells. Hepa1-6 cells were co-cultured with macrophages, and the number of invading Hepa1-6 cells was counted. Pre-treatment of macrophages with $GdCl_3$ before the Transwell assay markedly reduced the number of invading Hepa1-6 cells (P<0.001) (Fig. 4A and B). As $GdCl_3$ is able to either decrease the CD206 expression or induce the apoptosis of macrophages, it is necessary to clarify the precise role of CD206 in this phenomenon. RNA interference was used to downregulate the CD206 expression in RAW264.7 cells, and the knockdown efficacy was confirmed (Fig. 4D and E). Notably, knockdown of CD206 in RAW264.7 cells also reduced the capability of Hepa1-6 cell invasion (P<0.001). In contrast, IL-4-stimulated M2 macrophages enhanced the invasiveness of Hepa1-6 cells. These results suggest that $GdCl_3$ inhibited the invasiveness of HCC cells induced by the M2 macrophage phenotype of RAW264.7 cells and we speculated that CD206 may be involved in this process.

Downregulation of CD206 in M2 macrophages decreases the EMT of Hepa1-6 cells. Expression of the epithelial-mesenchymal transition (EMT)-related protein E-cadherin was reduced while N-cadherin, TWIST and Snail expression increased in the Hepa1-6 cells treated with IL-4-stimulated RAW264.7 macrophages. $GdCl_3$ treatment or downregulation of CD206 expression reversed this result (Fig. 4C and F).

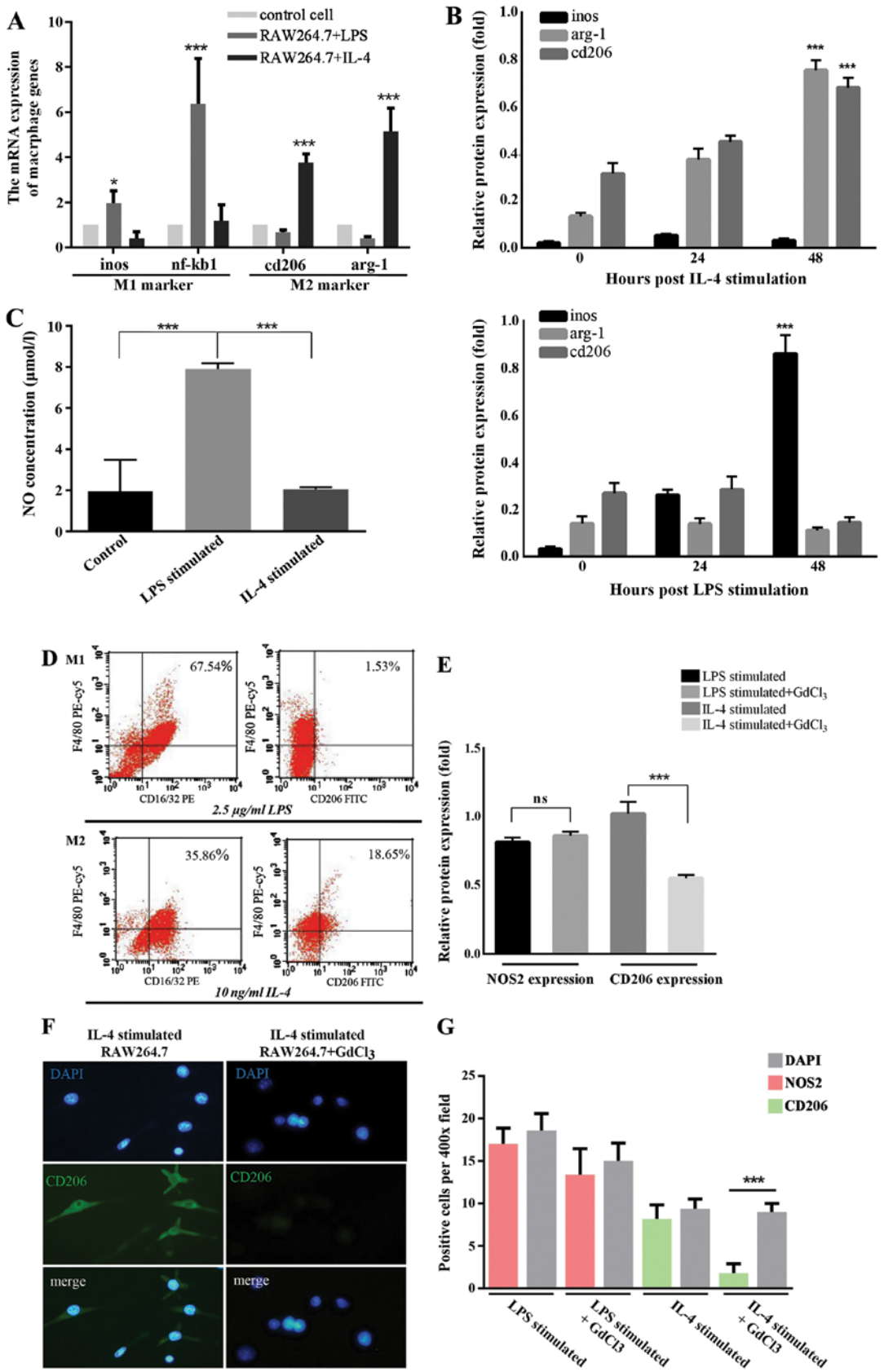

Figure 2. LPS- and IL-4-induced M1 and M2 macrophage phenotype conversion and the effects of $GdCl_3$ on CD206. RAW264.7 cells were incubated with 2.5 μg/ml LPS or 10 ng/ml IL-4. (A) mRNA expression of inos, NF-κB, cd206 and arg-1 were evaluated by quantitative RT-PCR 48 h after treatment. (B) Protein expression of iNOS, Arg-1 and CD206 was determined by western blotting at 0, 24 or 48 h after treatment, and is expressed as gray scale relative to the internal control β-actin. (C) NO concentration (μM) in cells stimulated with LPS or IL-4. (D) Expression of CD16/32 and CD206 was examined by flow cytometric analysis 48 h after treatment. RAW264.7 cells were incubated with 2.5 μg/ml LPS or10 ng/ml IL-4 in the presence or absence of 0.07 μg/μl $GdCl_3$ for 48 h. (E) Expression of NOS2, CD206 or GAPDH was measured by western blotting, and expressed as gray scale relative to the internal control GAPDH. (F) Cells were immunostained with anti-CD206 antibody. Nuclei were counterstained with DAPI. Magnification, x400. (G) The number of positive cells was counted. *P<0.05, **P<0.01, ***P<0.001.

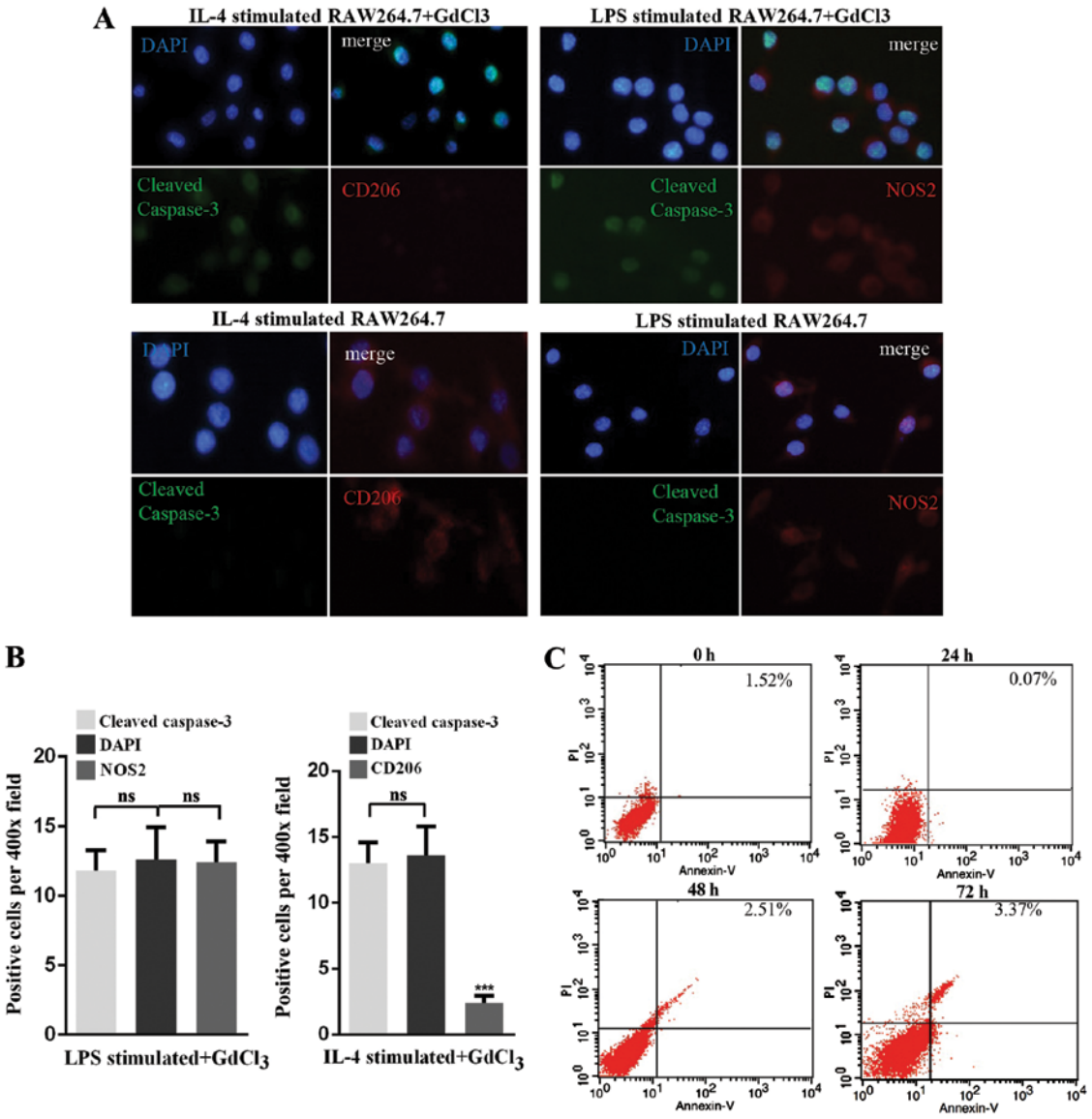

Figure 3. $GdCl_3$ induces cell apoptosis in M1 and M2 macrophage phenotypes induced by LPS and IL-4. RAW264.7 cells were incubated with 2.5 μg/ml LPS or 10 ng/ml IL-4 in the presence or absence of 0.07 μg/μl $GdCl_3$ for 48 h. (A) Cells were immunostained with anti-cleaved caspase-3 and anti-NOS2 or anti-CD206 antibodies. Nuclei were counterstained with DAPI. Magnification, x400. (B) The number of positive cells was counted. ***P<0.001; ns, no significance. (C) Apoptosis of Hepa1-6 cells was measured by Annexin V/PI staining followed by flow cytometric analysis.

These findings imply that CD206 may play a role in the EMT process.

Long-term treatment with $GdCl_3$ inhibits the progression of HCC and prevents liver fibrosis in mice. To evaluate the effects of $GdCl_3$ *in vivo*, DEN was used to establish a model of HCC in mice. We found that long-term treatment with $GdCl_3$ reduced tumor weight and volume of the DEN-treated mice (tumor volume, P<0.05; tumor weight, P<0.05) (Table III; Fig. 5A and B). Additionally, serum IL-6 and TNF-α levels, TGF-β1 and phospho-Smad3 expression in liver tissues were significantly elevated in the DEN-treated mice, while $GdCl_3$ therapy reduced the expression of IL-6, TNF-α, TGF-β1 and phospho-Smad3 (Fig. 5C and H). In addition, the animal survival data in the different groups demonstrated that long-term treatment of $GdCl_3$ was relatively safe (P<0.001) (Fig. 5E). Sirius red staining indicated the presence of liver fibrosis in the DEN-treated mice, which was attenuated following $GdCl_3$ treatment (Fig. 6B and C). No significant differences were found in the serum levels of ALT and AST between the DEN and DEN+$GdCl_3$ groups (Fig. 5D). Together, these results indicate that $GdCl_3$ inhibited the progression of HCC and prevented liver fibrosis in DEN-treated mice.

$GdCl_3$ downregulates the expression of CD206 in tumor tissues and promotes apoptosis of CD206-positive cells in vivo. Quantitative RT-PCR and western blot analysis demonstrated that both the mRNA and protein expression levels of CD206 were upregulated in the DEN-treated mice. $GdCl_3$ treatment reduced the upregulation of CD206 expression in tumor tissues (Fig. 5F and G). Even though the M1 macrophage-related iNOS expression was upregulated at 28 and 32 weeks after DEN injection, a reduced level of iNOS was observed at 36 weeks after DEN injection (data not shown).

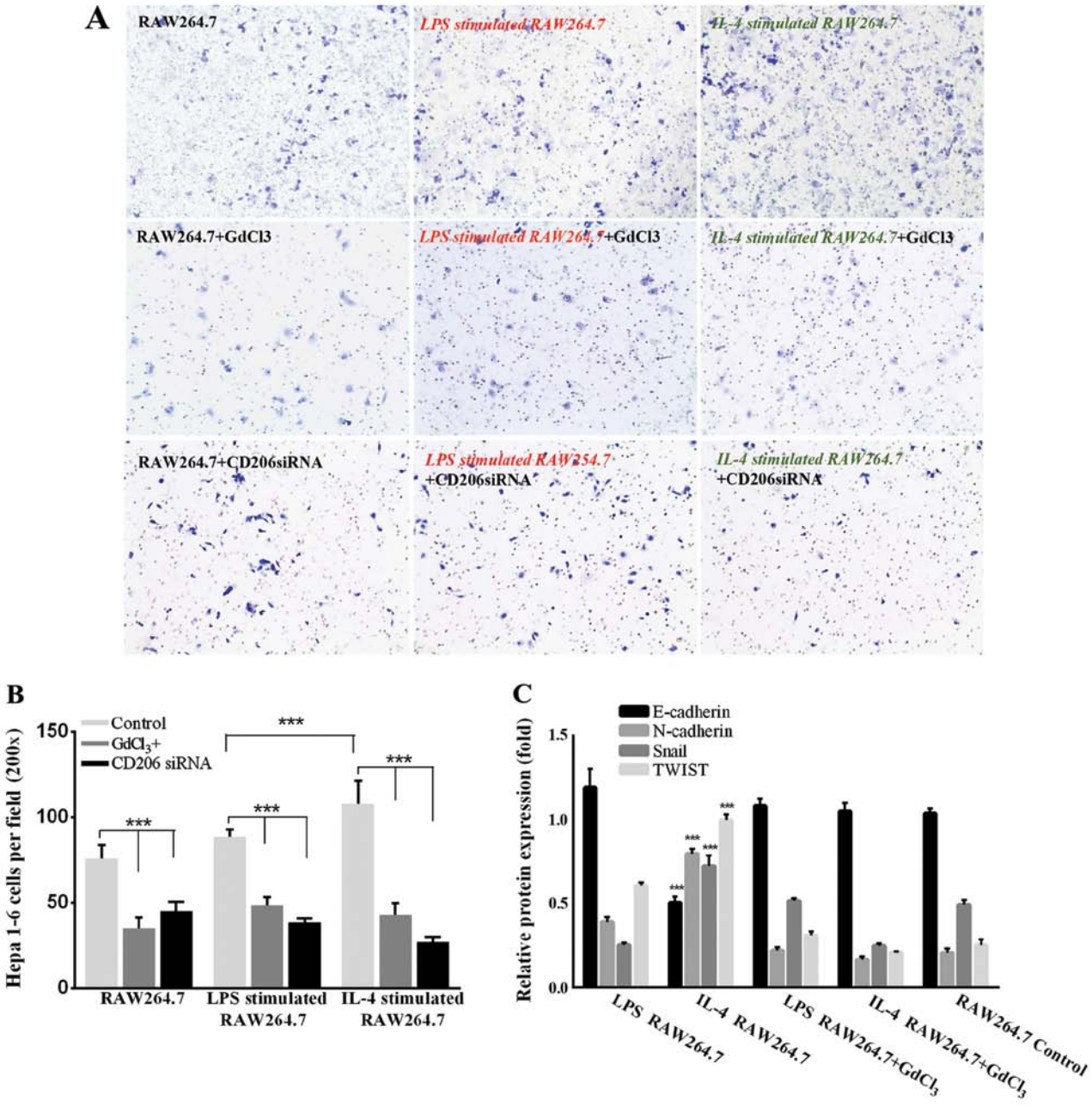

Figure 4. $GdCl_3$ suppresses the aggressive phenotype of HCC cells induced by the M2 macrophage phenotype of RAW264.7 cells. (A) Transwell Matrigel analysis of Hepa1-6 cells co-cultured with culture medium derived from RAW264.7 cells. RAW264.7 cells transfected with CD206 siRNA or control siRNA were stimulated with LPS or IL-4. (B) Invasive Hepa1-6 cells per field. (C) Expression of E-cadherin, N-cadherin, Snail, TWIST and GAPDH in HCC cells co-cultured with RAW264.7 cells following exposure to different treatments.

These data demonstrated that the majority of macrophages in the DEN-induced HCC had the M2 phenotype. At 40 weeks after DEN injection, F4/80-positive cells expressed CD206, and cleaved caspase-3 expression was barely detectable in these cells (Fig. 6A). We found that $GdCl_3$ treatment reduced the number of cells expressing CD206 and iNOS and increased the number of cells expressing cleaved caspase-3, indicating that $GdCl_3$ treatment could induce macrophage apoptosis in the mouse liver. In addition, as shown in Fig. 6D and E, $GdCl_3$ treatment downregulated the expression of CD31, CD206 and the CD31-associated MVD value in liver tissues, revealing that it also had the ability to inhibit tumor angiogenesis.

Discussion

The clinical association of TAMs in the tumor microenvironment with poor prognosis has been extensively documented in numerous types of cancers (22). TAMs consist primarily of a polarized M2 macrophage population and promote proliferation, migration and invasion of tumor cells by secreting growth factors, proangiogenic factors and metalloproteinase (23,24). The mannose receptor 1, or CD206, plays a key role in the phagocytosis of pathogens, antigen presentation, intracellular signaling and resolution of inflammation (25). Previous studies have detected increased expression of the mannose

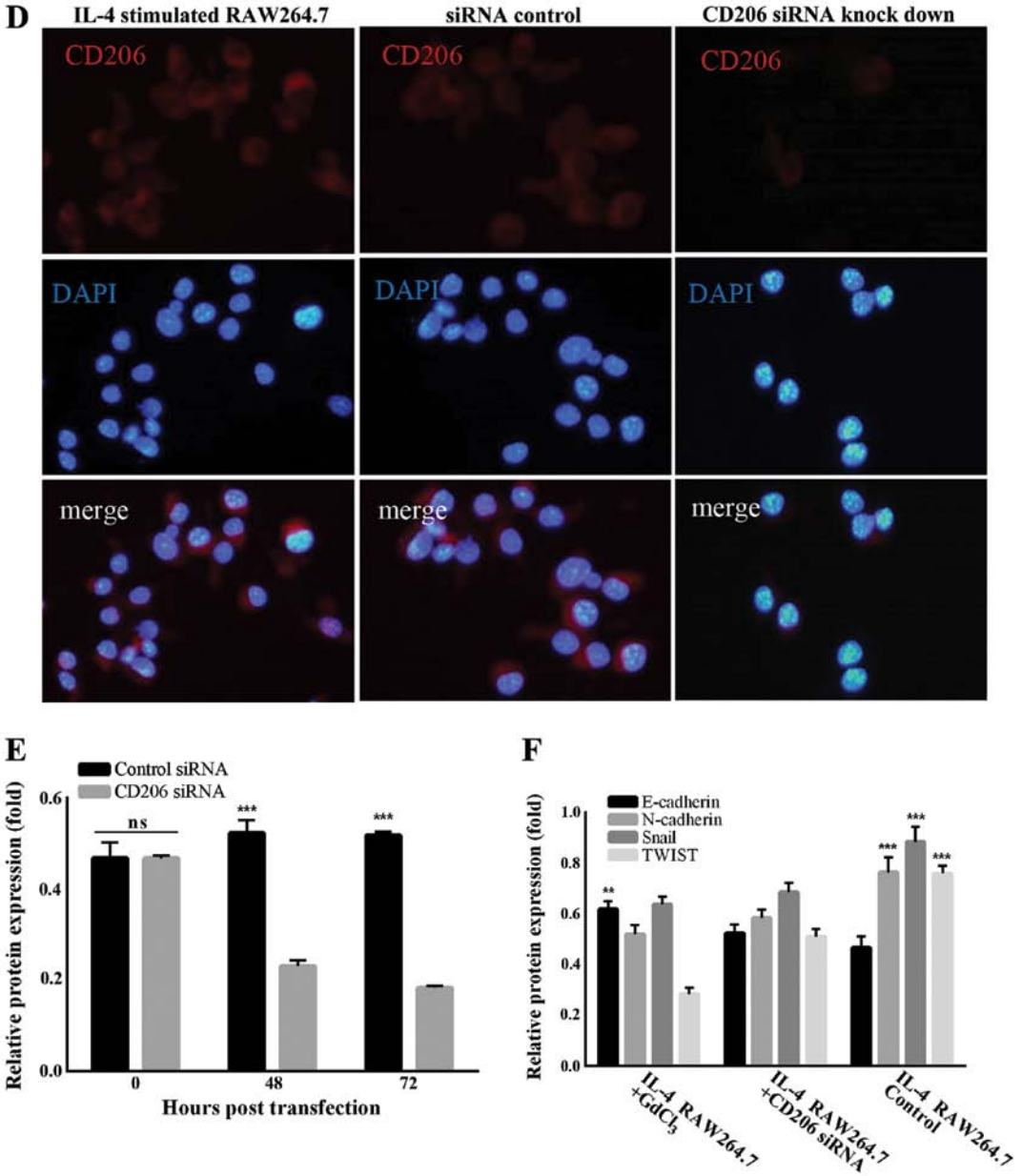

Figure 4. Continued. CD206 knockdown efficacy as determined by (D) immunostaining and (E) western blotting. (F) Expression of E-cadherin, Snail, TWIST and GAPDH in HCC cells co-cultured with IL-4-stimulated RAW264.7 cells treated with $GdCl_3$, CD206 siRNA or control. Protein expression levels in (C-F) are expressed as gray scale relative to the internal control GAPDH. ***P<0.001.

receptor CD206 in TAMs isolated from breast tumor tissues (23,26). However, the relationship between CD206 expression and HCC prognosis has not yet been elucidated. In the present study, we showed that CD206 expression is an independent factor associated with the prognosis of HCC patients, with elevated levels of expression being associated with poor prognosis. In addition, increased CD206 expression was observed in HCC tissues compared with peri-carcinoma tissues and in cultured macrophages stimulated by IL-4.

$GdCl_3$ is an MRI contrast agent which is widely used at present and whose safety has been evaluated (27,28). We found that high dosages of $GdCl_3$ markedly suppressed the proliferation of macrophages. However, at its IC_{10} (0.07 $\mu g/\mu l$) concentration, CD206 expression was suppressed efficiently in TAMs. In addition, at this dosage, $GdCl_3$ inhibited the aggressiveness of Hepa1-6 cells induced by the M2 macrophage phenotype of RAW264.7 cells. After CD206 expression was downregulated by RNAi for comparison, the cells lost their ability to increase the aggressiveness of Hepa1-6 HCC cells, as observed following $GdCl_3$ treatment.

To further elucidate the role of CD206 and the therapeutic value of $GdCl_3$, we investigated the epithelial-mesenchymal transition properties of Hepa1-6 cells. EMT is a process by which epithelial cells lose their polarity and cell-cell adhesion properties and gain migratory and invasive abilities to become mesenchymal stem cells (29). The transcription factor TWIST is known to regulate tumor metastasis, and plays a crucial role in mediating the migration and invasion of HCC cells (30). In accordance with our findings, we found that E-cadherin was downregulated while TWIST, N-cadherin, and Snail

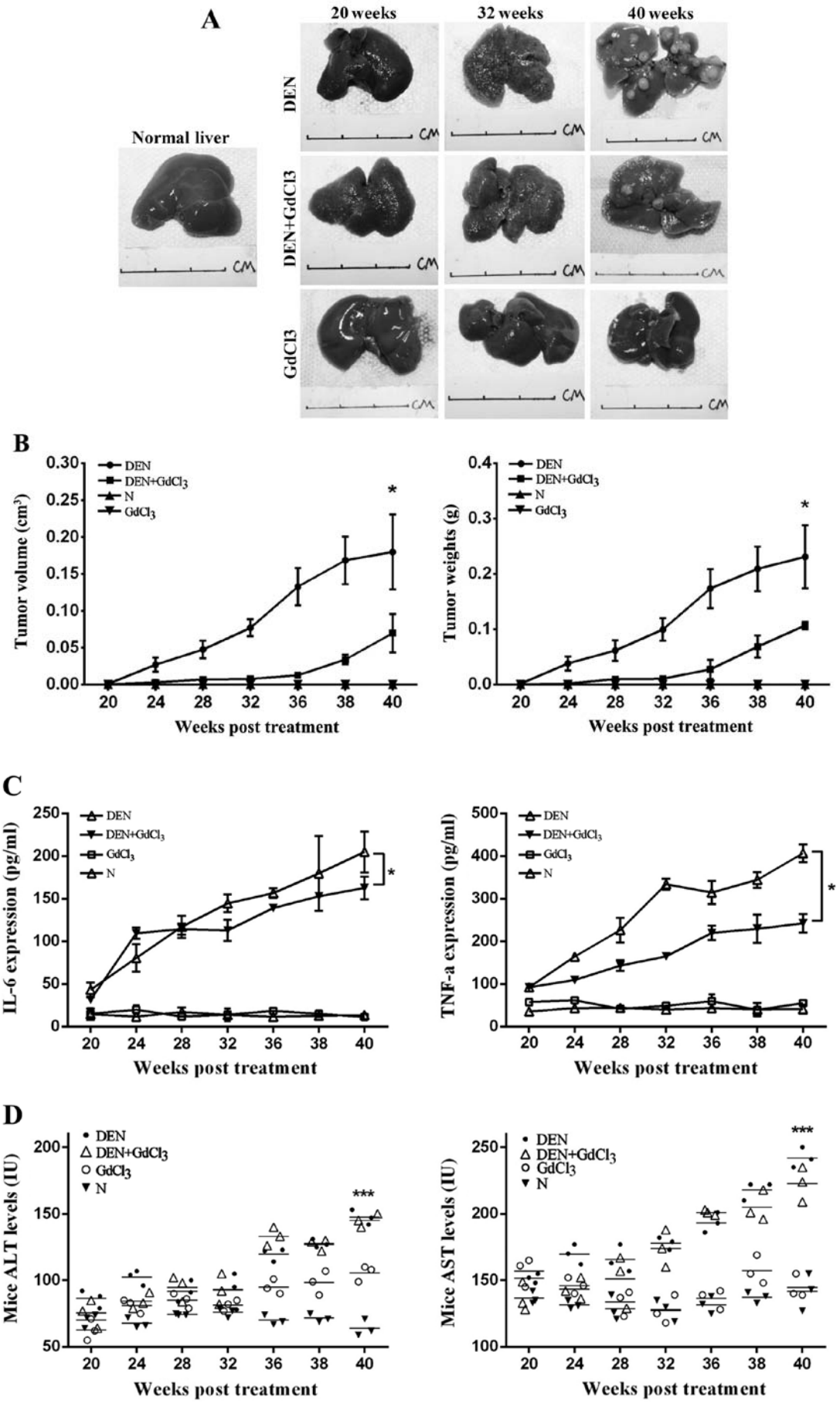

Figure 5. $GdCl_3$ inhibits tumor growth and reduces mortality in HCC mice. (A) Gross observation of liver tumor formation and the effectiveness of $GdCl_3$ treatment in DEN-injected mice. (B) Tumor volume and tumor weight. (C) Cytokine level. (D) ALT and AST levels were analyzed, and are expressed as gray scale relative to the internal control GAPDH.

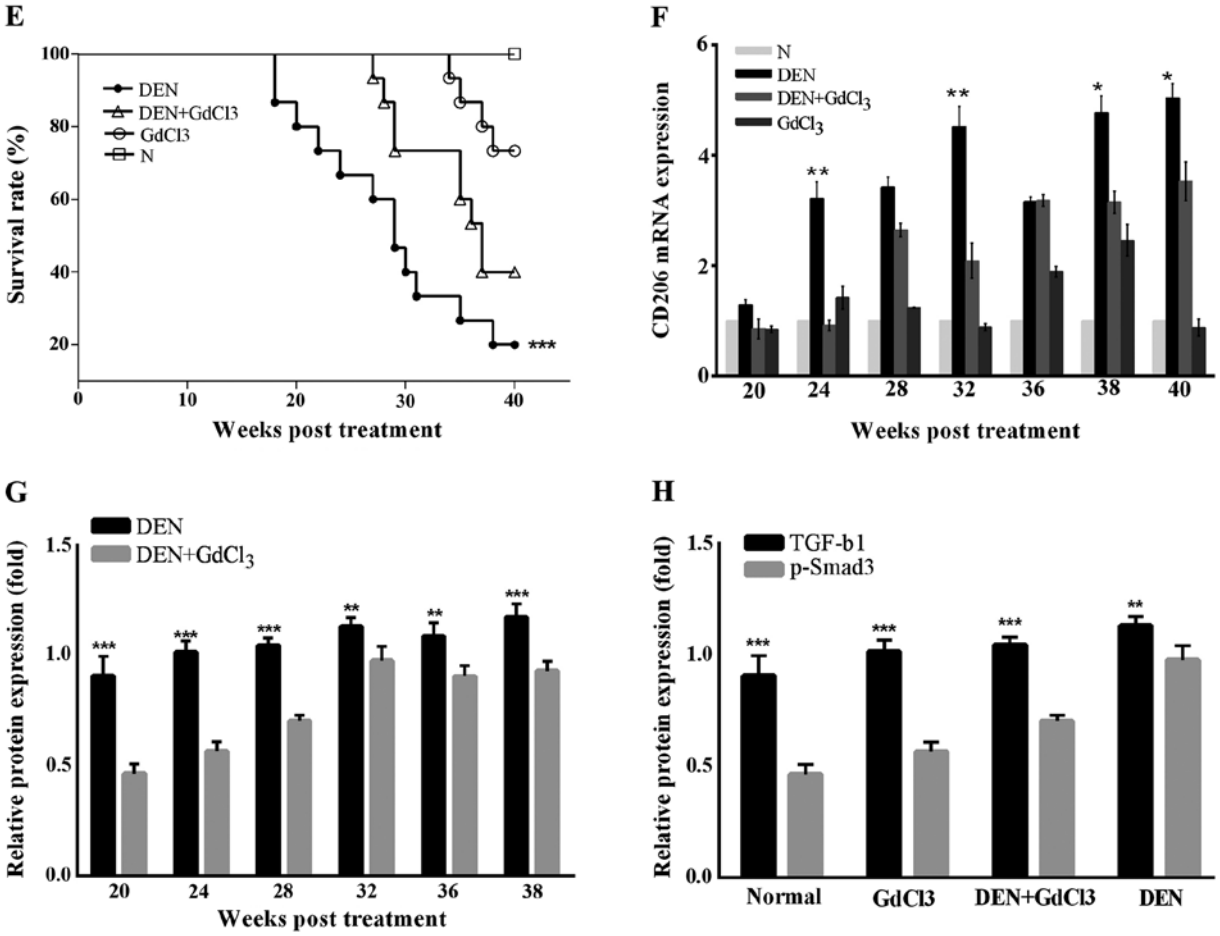

Figure 5. Continued. (E) Animal survival rate. (F) mRNA and (G) protein expression of CD206. (H) Protein expression of TGF-1β and p-Smad3 in mice was analyzed, and expressed as gray scale relative to the internal control GAPDH. **P<0.01, ***P<0.001.

Table III. Tumor inhibition rate (TIR) and tumor volume growth rate (TVGR) of tumor-bearing mice at week 40 (n=4 in each group, data are expressed as mean ± SD).

Group	Average tumor weight	TIR (%)[a]	Average tumor volume (cm^3)	TVGR (%)[a]
DEN	0.231±0.057	-	0.180±0.507	-
DEN+$GdCl_3$	0.107±0.068[b]	53.7	0.070±0.261[b]	38.8

[a]TIR = [(Average tumor weight of DEN group - Average tumor weight of DEN+$GdCl_3$ group)/Average tumor weight of DEN group] x 100%. TVGR = ($V_{tumor\ DEN+GdCl_3}/V_{tumor\ DEN}$) x 100%. [b]P<0.05, compared with average tumor weight/volume of DEN group.

were upregulated in Hepa1-6 cells which undergo EMT when co-cultured with M2 cells. Interference of the pharmacological treatment with $GdCl_3$ of macrophages or by silencing of CD206 expression efficiently reversed the downregulation of E-cadherin and the upregulation of TWIST, Snail, and N-cadherin, indicating that $GdCl_3$ inhibited the RAW264.7-induced aggressiveness of HCC cells mainly by inhibiting the expression of CD206 in the M2 macrophage phenotype. In the mouse HCC model, a long-term injection of $GdCl_3$ efficiently inhibited the progression of HCC. Fibrosis-associated TGF-β1 and phospho-Smad3 expression was reversed by $GdCl_3$ treatment. We found that there were no significant differences in the serum levels of ALT and AST between the DEN and DEN+$GdCl_3$ groups. We speculated that although $GdCl_3$ inhibited the DEN-induced HCC and fibrosis, the long-term use of $GdCl_3$ might increase the ALT and AST levels (particularly ALT levels). This could be considered as a side-effect of $GdCl_3$. It was reported that the mannose receptor family contains the fibronectin type II repeat domain, which binds to collagens (type I-III) with high affinity. After binding, the mannose receptor internalizes collagen in macrophages and liver sinusoidal cells, which plays a crucial role in fibrosis (31). The expression of CD206 was downregulated after $GdCl_3$ treatment in the mouse liver. Remission of liver fibrosis was possible by downregulation of CD206 expression in tumor tissues and the promotion of apoptosis of CD206-positive

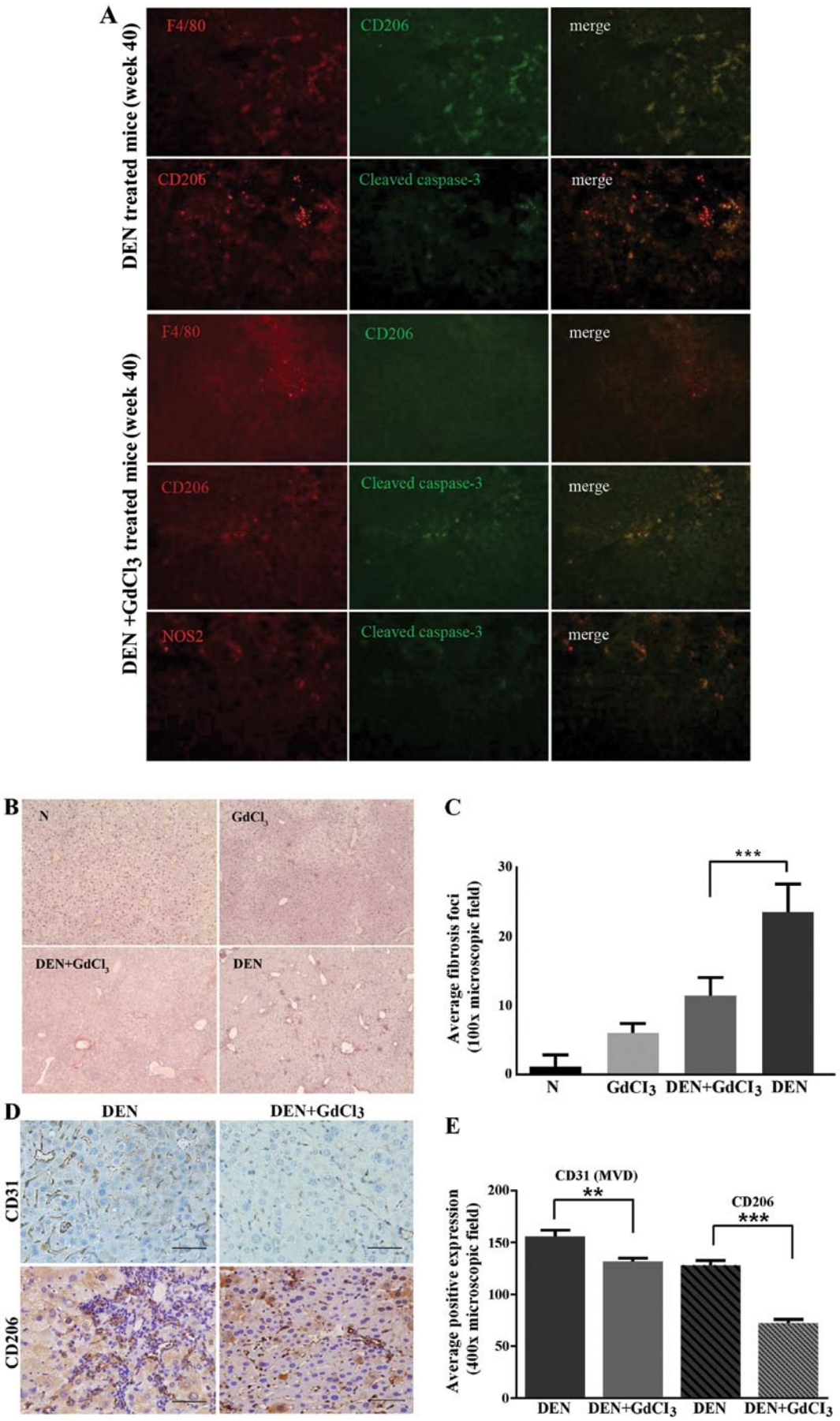

Figure 6. $GdCl_3$ promotes the apoptosis of CD206-positive cells *in vivo*. (A) The expression of F4/80, CD206, cleaved caspase-3 and NOS-2 in liver tissues was examined by immunostaining 40 weeks after injection of DEN. (B) Sirius red staining in liver sections. (C) Average fibrosis foci in liver sections determined by Sirius red staining (***P<0.001, n=6). (D) CD31 and CD206 expression. Scale bar, 50 μm. (E) Quantified data of CD31 and CD206 expression. **P<0.01; ***P<0.001. n=12.

M2 cells in the DEN-induced HCC mice. Ruttinger *et al* (32) reported that a single dose of $GdCl_3$ elevated the serum levels of TNF-α and IL-6 in rats. However, in the present study, we did not detect a significant elevation in the above inflammatory factors in mouse serum, possibly due to a difference in treatment regimens and detection analysis.

CD206 is not secreted. We found that downregulation of CD206 in M2 macrophages inhibited its pro-tumorigenesis functions, possibly by affecting cytokine secretion. For instance, it has been reported that the HEK293 cells co-transfected with CD206 and human Toll-like receptor 2 cDNA are able to secrete IL-8, whereas cells transfected with either receptor alone are not (33). IL-8 is secreted by proangiogenic macrophages in cancer (34). In the present study, we showed for the first time that $GdCl_3$ suppressed the malignant potential of HCC *in vitro* and *in vivo* mainly by inhibiting CD206 activity. Importantly, long-term administration of $GdCl_3$ only slightly affects liver function or animal survival, suggesting that it may be a safe therapeutic agent which could yield a promising strategy for the treatment of HCC.

Acknowledgements

The present study was supported by the National Natural Science Foundation (grant nos. 81071882 and 81372481) and the National Key Clinical Specialties Construction Program of China.

References

1. Thorgeirsson SS and Grisham JW: Molecular pathogenesis of human hepatocellular carcinoma. Nat Genet 31: 339-346, 2002.
2. Boltjes A, Movita D, Boonstra A and Woltman AM: The role of Kupffer cells in hepatitis B and hepatitis C virus infections. J Hepatol 61: 660-671, 2014.
3. Wu J, Li J, Salcedo R, Mivechi NF, Trinchieri G and Horuzsko A: The proinflammatory myeloid cell receptor TREM-1 controls Kupffer cell activation and development of hepatocellular carcinoma. Cancer Res 72: 3977-3986, 2012.
4. Mantovani A, Sozzani S, Locati M, Allavena P and Sica A: Macrophage polarization: Tumor-associated macrophages as a paradigm for polarized M2 mononuclear phagocytes. Trends Immunol 23: 549-555, 2002.
5. Mantovani A, Allavena P, Sica A and Balkwill F: Cancer-related inflammation. Nature 454: 436-444, 2008.
6. Pollard JW: Trophic macrophages in development and disease. Nat Rev Immunol 9: 259-270, 2009.
7. Sica A, Allavena P and Mantovani A: Cancer related inflammation: The macrophage connection. Cancer Lett 267: 204-215, 2008.
8. Heusinkveld M and van der Burg SH: Identification and manipulation of tumor associated macrophages in human cancers. J Transl Med 9: 216, 2011.
9. Mantovani A, Vecchi A and Allavena P: Pharmacological modulation of monocytes and macrophages. Curr Opin Pharmacol 17: 38-44, 2014.
10. Germano G, Frapolli R, Belgiovine C, Anselmo A, Pesce S, Liguori M, Erba E, Uboldi S, Zucchetti M, Pasqualini F, *et al*: Role of macrophage targeting in the antitumor activity of trabectedin. Cancer Cell 23: 249-262, 2013.
11. Huang W, Metlakunta A, Dedousis N, Zhang P, Sipula I, Dube JJ, Scott DK and O'Doherty RM: Depletion of liver Kupffer cells prevents the development of diet-induced hepatic steatosis and insulin resistance. Diabetes 59: 347-357, 2010.
12. Ide M, Kuwamura M, Kotani T, Sawamoto O and Yamate J: Effects of gadolinium chloride ($GdCl_3$) on the appearance of macrophage populations and fibrogenesis in thioacetamide-induced rat hepatic lesions. J Comp Pathol 133: 92-102, 2005.
13. Hardonk MJ, Dijkhuis FW, Hulstaert CE and Koudstaal J: Heterogeneity of rat liver and spleen macrophages in gadolinium chloride-induced elimination and repopulation. J Leukoc Biol 52: 296-302, 1992.
14. Rinnenthal JL, Goebel HH, Preuße C, Lebenheim L, Schumann M, Moos V, Schneider T, Heppner FL and Stenzel W: Inflammatory myopathy with abundant macrophages (IMAM): The immunology revisited. Neuromuscul Disord 24: 151-155, 2014.
15. Roca H, Varsos ZS, Sud S, Craig MJ, Ying C and Pienta KJ: CCL2 and interleukin-6 promote survival of human $CD11b^+$ peripheral blood mononuclear cells and induce M2-type macrophage polarization. J Biol Chem 284: 34342-34354, 2009.
16. Wang Y, Wang YP, Zheng G, Lee VW, Ouyang L, Chang DH, Mahajan D, Coombs J, Wang YM, Alexander SI, *et al*: Ex vivo programmed macrophages ameliorate experimental chronic inflammatory renal disease. Kidney Int 72: 290-299, 2007.
17. Gao XF, Li QL, Li HL, Zhang HY, Su JY, Wang B, Liu P and Zhang AQ: Extracts from *Curcuma zedoaria* inhibit proliferation of human breast cancer cell MDA-MB-231 in vitro. Evid Based Complement Alternat Med 2014: 730678, 2014.
18. Kyriazis AP, Koka M and Vesselinovitch SD: Metastatic rate of liver tumors induced by diethylnitrosamine in mice. Cancer Res 34: 2881-2886, 1974.
19. Zhao YZ, Dai DD, Lu CT, Lv HF, Zhang Y, Li X, Li WF, Wu Y, Jiang L, Li XK, *et al*: Using acoustic cavitation to enhance chemotherapy of DOX liposomes: Experiment in vitro and in vivo. Drug Dev Ind Pharm 38: 1090-1098, 2012.
20. Tartis MS, McCallan J, Lum AF, LaBell R, Stieger SM, Matsunaga TO and Ferrara KW: Therapeutic effects of paclitaxel-containing ultrasound contrast agents. Ultrasound Med Biol 32: 1771-1780, 2006.
21. Weidner N, Semple JP, Welch WR and Folkman J: Tumor angiogenesis and metastasis - correlation in invasive breast carcinoma. N Engl J Med 324: 1-8, 1991.
22. Martinez FO, Helming L and Gordon S: Alternative activation of macrophages: An immunologic functional perspective. Annu Rev Immunol 27: 451-483, 2009.
23. Luo Y, Zhou H, Krueger J, Kaplan C, Lee SH, Dolman C, Markowitz D, Wu W, Liu C, Reisfeld RA, *et al*: Targeting tumor-associated macrophages as a novel strategy against breast cancer. J Clin Invest 116: 2132-2141, 2006.
24. Lawrence T and Natoli G: Transcriptional regulation of macrophage polarization: Enabling diversity with identity. Nat Rev Immunol 11: 750-761, 2011.
25. Gazi U and Martinez-Pomares L: Influence of the mannose receptor in host immune responses. Immunobiology 214: 554-561, 2009.
26. Zhang H, Luo M, Jin Z, Wang D, Sun M, Zhao X, Zhao Z, Lei H, Li M and Liu C: Expression and clinicopathological significance of FSIP1 in breast cancer. Oncotarget 6: 10658-10666, 2015.
27. Warntjes JB, Tisell A, Landtblom AM and Lundberg P: Effects of gadolinium contrast agent administration on automatic brain tissue classification of patients with multiple sclerosis. AJNR Am J Neuroradiol 35: 1330-1336, 2014.
28. Wong TC: Cardiovascular magnetic resonance imaging of myocardial interstitial expansion in hypertrophic cardiomyopathy. Curr Cardiovasc Imaging Rep 7: 9267, 2014.
29. Kong D, Li Y, Wang Z and Sarkar FH: Cancer stem cells and epithelial-to-mesenchymal transition (EMT)-phenotypic cells: are they cousins or twins? Cancers (Basel) 3: 716-729, 2011.
30. Matsuo N, Shiraha H, Fujikawa T, Takaoka N, Ueda N, Tanaka S, Nishina S, Nakanishi Y, Uemura M, Takaki A, *et al*: Twist expression promotes migration and invasion in hepatocellular carcinoma. BMC Cancer 9: 240, 2009.
31. Martinez-Pomares L: The mannose receptor. J Leukoc Biol 92: 1177-1186, 2012.
32. Rüttinger D, Vollmar B, Wanner GA and Messmer K: In vivo assessment of hepatic alterations following gadolinium chloride-induced Kupffer cell blockade. J Hepatol 25: 960-967, 1996.
33. Tachado SD, Zhang J, Zhu J, Patel N, Cushion M and Koziel H: Pneumocystis-mediated IL-8 release by macrophages requires coexpression of mannose receptors and TLR2. J Leukoc Biol 81: 205-211, 2007.
34. Dalton HJ, Armaiz-Pena GN, Gonzalez-Villasana V, Lopez-Berestein G, Bar-Eli M and Sood AK: Monocyte subpopulations in angiogenesis. Cancer Res 74: 1287-1293, 2014.